ACS APPLIED MATERIALS & INTERFACES

Energy, Environmental, and Catalysis Applications

A High-Performance and Recyclable Al-Air Coin Cell Based on Eco-Friendly Chitosan Hydrogel Membranes

Yisi Liu, Qian Sun, Xiaofei Yang, Jianneng Liang, Biqiong Wang, Alicia Koo, Ruying Li, Jie Li, and Xueliang Sun

ACS Appl. Mater. Interfaces, **Just Accepted Manuscript** • DOI: 10.1021/acsami.8b04974 • Publication Date (Web): 18 May 2018

ACS Publications

is published by the American Chemical Society. 1155 Sixteenth Street N.W., Washington, DC 20036

A High-Performance and Recyclable Al-Air Coin Cell Based on Eco-Friendly Chitosan Hydrogel Membranes

Yisi Liu [1, a, b], Qian Sun [1, b], Xiaofei Yang [b, c], Jianneng Liang [b], Biqiong Wang [b], Alicia Koo [b], Ruying Li [b], Jie Li [a*], Xueliang Sun [b*]

[a] School of Chemistry and Chemical Engineering, Central South University, Changsha 410083 China

[b] Department of Mechanical and Materials Engineering, University of Western Ontario, London, Ontario N6A 5B9, Canada

[c] Division of Energy Storage, Dalian Institute of Chemical Physics, Chinese Academy of Sciences, Dalian 116023, PR China

[*]Corresponding author.

[*]E-mail addresses: lijieliu@csu.edu.cn, xsun@eng.uwo.ca

Yisi Liu and Qian Sun contributed equally to this work.

Abstract

Aluminum-air batteries are a promising power supply for electronics due to its low cost and high energy density. However, portable coin-type Al-air batteries operating under ambient air condition for small electronic appliances have rarely been reported. Herein, coin cell-type Al-air batteries using cost-effective and eco-friendly chitosan hydrogel membranes modified by SiO_2, SnO_2, and ZnO have been prepared and assembled. The Al-air coin cell employing chitosan hydrogel membrane containing 10 wt.% SiO_2 as a separator exhibits better discharge performance with a higher flat voltage plateau, longer discharge duration, and higher power density than the cells using a chitosan hydrogel membrane containing SnO_2 or ZnO. Moreover, we also demonstrate that the presented Al-air coin cell can be recycled by a series of eco-friendly procedures using food grade ingredients, resulting in recycled products that are environmentally safe and ready for reuse. The Al-air coin cell adopting a recycled cathode from a fully discharged Al-air coin cell using the above-mentioned procedure has shown comparable performance to cells assembled with a new cathode. With these merits of enhanced electrochemical performance and recyclability, this new Al-air coin cell with modified chitosan hydrogel membrane can find wide applications for powering portable and small-size electronics.

Key words: Al-air battery, chitosan, environmental-friendly, hydrogel, recycle

1. Introduction

Extensive research interest and effort have been focused on aqueous metal-air batteries, such as zinc (Zn)-air, magnesium (Mg)-air, and aluminum (Al)-air batteries due to their high theoretical energy densities .[1-4] Among these metal-air batteries, the Al-air battery has been considered as an inexpensive, safe, and environmentally friendly power supply with high recyclability. As an anode, Al has very high theoretical specific capacity of 2.98 Ah g^{-1}_{Al}, which is second only to lithium (3.86 Ah g^{-1}_{Li}) and is much higher than that of magnesium (2.20 Ah g^{-1}_{Mg}) and zinc (0.82 Ah g^{-1}_{Zn}), [5-7] making Al-air batteries highly attractive. The conventional Al-air battery is composed of an aluminum anode, an air cathode, and a suitable electrolyte, such as aqueous sodium hydroxide (NaOH), potassium hydroxide (KOH) or sodium chloride (NaCl) solutions. As of now, Al-air battery packs have already found large scale applications, such as in electric vehicles (EVs). However, a facile design for Al-air batteries for applications in protable or consumable electrionics, where the coin-type battery configuration is most commonly adopted has not yet been widely explored. Moreover, traditional Al-air batteries have risk of large leakage of alkaline electrolyte, and the fabrication of air cathodes is complicated. Therefore, to further extend the applications and simplify assembly process of Al-air batteries, a novel coin-type design must be developed.

A core component of the coin-type cell is the separator, also known as the electrolyte membrane. Ionic conductivity and cost are the most critical concerns of separators. Polymer membranes have been widely employed in electrochemical

energy conversion or storage devices. [8-9] Up to now, Nafion® perfluorinated membranes, a type of cation exchange membrane, have been the most commonly used separators for aqueous electrolytes in polymer electrolyte fuel cells (PEFCs), [10-11] direct borohydride fuel cells (DBFCs), [12-13] and direct methanol fuel cells (DMFCs). [14-15] Nafion® is also used as an ionic conductor and electrode binder for cathodes which provides mechanical support for catalyst particles, and enhances dispersion of catalyst particles in the catalyst layer in these fuel cells. [16] However, the high cost of Nafion® can be an obstacle for the realization of affordable Al-air batteries. Therefore, developing effective and low-cost polymer materials as separators for aqueous batteries is highly desired. [17-18]

Hydrogels have been considered to be promising candidates as low cost membrane materials for aqueous batteries, [3, 48] which are composed of three-dimensional networks that absorb and retain large amounts of water within their solid polymeric matrices. Recently, An et al. proposed an agar chemical hydrogel electrode binder to enhance mass transport. [19] Chemical hydrogels are formed by a chemical reaction between a polymer and a cross-linking reagent. [20] Polymer hydrogels, such as poly vinyl alcohol (PVA), poly ethylene oxide (PEO), and poly acrylic acid (PAA) based hydrogels [21-24] have been reported as solid-state electrolytes in electrochemical devices. For instance, Peng et al. reported all-solid-state fiber-shaped Zn-air and Al-air batteries with a hydrogel polymer electrolyte composed of PVA, PEO, and KOH. [25-26] The batteries are flexible, stretchable, and exhibit good electrochemical performances. Zeng et al. [27] fabricated a quasi-solid-state

Zn-MnO_2@PEDOT battery using PVA/$ZnCl_2$/$MnSO_4$ gel as the electrolyte, which resulted in remarkable capacity, power density and excellent durability, while also remaining highly rechargeable. Among gel polymer electrolytes (GPEs), hydrogels prepared from natural-source carbohydrate polymers (cellulose, starch, chitosan, agarose) have been extensively studied for electrochemical devices. [28-30] Advantages of using such polymers include the easily obtained starting materials from renewable, inexpensive, and eco-friendly sources, all while maintaining high conductivity. A carbohydrate polymer of interest is, chitosan which is a biodegradable, biocompatible, natural polymer derived from chitin [poly(N-acetyl-d-glucosamine)] by deacetylation. Chitin, which is present in the exoskeleton of arthropods, is second only to cellulose as the most abundant natural polymer. [31] Chitosan is weakly alkaline and is soluble in dilute weak organic acid solutions to form chitosan hydrogels, which can be cast into gel beads, membranes and other forms by physical modifications. For instance, Choudhury et al. [32] reported studies on using chitosan-KOH as a polymer electrolyte membrane in direct borohydride fuel cells (DBFCs). The DBFCs exhibited peak power density values of about 81 and 72 mW cm^{-2} at corresponding current density values of about 85 and 73 mA cm^{-2}, respectively. In another paper, Ma et al. prepared phosphate chitosan (CsP) and triphosphate chitosan (CsTP) hydrogel membranes as polymer electrolyte for use in DBFCs, which showed significantly high power density and better stability compared to Nafion®-based DBFCs. [33] However, the utilization of chitosan-based hydrogel membranes in metal-air batteries remains unexplored. In the Al-air coin construction, maybe they can be used as separators.

In this study, chitosan-based hydrogel membranes were prepared, characterized, and adopted in coin-type Al-air batteries as separators. Considering the severe anodic corrosion, various metal oxides (SiO_2, SnO_2, and ZnO) were added to modify the chitosan membranes to inhibit the corrosion rate. We compared the discharge performance of coin cells with SiO_2-chitosan, SnO_2-chitosan, and ZnO-chitosan membranes. The coin cell with 10 wt.% SiO_2-chitosan membrane exhibits the best discharge performance with a prominent capacity of 288.5 mAh g^{-1}_{Al} at a current density of 1.0 mA cm^{-2}. Additionally, a series of simple procedures were developed to recycle the components of Al-air coin cells after discharge. The final products after recycling are environmentally safe and can be reused or arbitrarily disposed.

2. Experimental

2.1 Membrane preparation

2 g of chitosan powder was dissolved in 100 mL of 2% (v/v) aqueous solution of acetic acid and vigorously stirred for 24 h to form a clear gel. The solution was poured into a Teflon mold then dried in air, first at room temperature then at 60 ℃ for 24 h to obtain a pristine chitosan (CS) membrane. The preparation process of the chitosan membrane is illustrated schematically in **Figure 1**. Chitosan membranes containing metal oxides were synthesized with the above procedure with the addition of 0.2 g of SiO_2, SnO_2, or ZnO powders into the aqueous solution to form 10 wt.% SiO_2-chitosan, 10 wt.% SnO_2-chitosan, and 10 wt.% ZnO-chitosan hydrogel membranes, respectively. SiO_2-chitosan hydrogel membranes with different mass

ratios of SiO_2 and chitosan (5 wt.%, 10 wt.%, and 15 wt.%) were also prepared using the above method, denoted as 5%-SiO_2-CS-HGM, 10%-SiO_2-CS-HGM, and 15%-SiO_2-CS-HGM.

2.2 Corrosion mechanism

In alkaline solution, the Al anode reacts with KOH to form $Al(OH)_3$, the most common corrosion product:

$$Al + 3OH^- \rightarrow Al(OH)_3 + 3e^- \quad (2\text{-}1)$$

Side reactions between the SiO_2, SnO_2, and ZnO metal oxides present in CS-HGMs, and KOH are summarized as follows:

$$SiO_2 + 2OH^- \rightarrow SiO_3^{2-} + H_2O \quad (2\text{-}2)$$

$$SnO_2 + 2OH^- \rightarrow SnO_3^{2-} + H_2O \quad (2\text{-}3)$$

$$ZnO + H_2O + 2OH^- \rightarrow Zn(OH)_4^{2-} \quad (2\text{-}4)$$

The SiO_3^{2-} and SnO_3^{2-} products are well known as corrosion inhibitors in the Al-air system [5, 34-36]. Whereas, the corrosion inhibition of ZnO is diminished by the reaction between ZnO and KOH (Equation 2-4). SiO_3^{2-} ions can inhibit the pitting of the Al alloy to promote deactivation [36]. SnO_3^{2-} can decrease the overpotential and self-corrosion rate in alkaline solution [4]. In this work, effective corrosion inhibitors were produced by the reaction between CS-HGMs and KOH, improving the practical efficiency of Al-air coin cells.

2.3 Ionic conductivity measurement

The ionic conductivity of chitosan-based membranes was measured in a two-point-probe conductivity cell at room temperature by electrochemical impedance

spectroscopy (EIS). Nyquist plots were recorded by a Gamry Electrochemical system in the frequency range of 100 mHz and 100 kHz with an AC voltage of 5 mV. Before each conductivity measurement, the membranes were equilibrated for 5 minutes in 2 M aqueous NaOH solution then dried. Ionic conductivity (σ) was calculated by the following equation: [37]

$$\sigma = \frac{L}{R_b A} \quad (2\text{-}5)$$

Where σ (S cm^{-1}) is the membrane conductivity, L (cm) is the membrane thickness, A (cm^2) is the geometric area of the membrane, and R_b is the bulk resistance calculated from the high-frequency intercept on the real axis of the Nyquist plot.

2.4 Fabrication and discharge tests of aluminum-air coin cells

The air electrode was fabricated by coating catalyst paste on carbon paper (Toray, TGP-H-60) with a diameter of 10 mm, which was then dried in a vacuum oven at 60 ℃ for 2 h for a loading of approximately 1.5 mg cm^{-2}. The catalyst paste is composed of 10 mg of the Mn_3O_4/C catalyst dispersed in a mixture of 67 μL of 5 wt.% Nafion (D-521, Alfar Aesar) and 1.0 mL of isopropyl alcohol. The Al-air coin battery (**Figure S1**) was fabricated with a 1 cm × 1 cm aluminum foil (99.997 %, 0.25 mm, Alfa Aesar) as the anode, a hydrogel membrane and a piece of glass microfiber with the diameter of 16 mm (Whatman, Grade 934-AH) dual layer separator, a carbon paper coated with Mn_3O_4/C catalyst as cathode, and a 2 mol L^{-1} KOH aqueous solution (~ 1 mL) as the electrolyte. The Mn_3O_4/C catalyst was synthesized as follows [38]: commercial Mn_3O_4 powders were ultrasonicated in a suspension of Vulcan XC-72 carbon in ethanol. The solution was then transferred into a 50 mL Teflon-lined

autoclave, and heated at 150 °C for 3 h. The precipitate was collected and purified by centrifuging with deionized water and ethanol for several times. Finally, the as-prepared product was dried in a vacuum oven at 60 ˚C for 12 h.

The cell discharge tests were carried out by a multichannel battery testing system (LANHE CT2001A). The cells were discharged galvanostatically to a cutoff voltage of 0 V at room temperature under ambient condition. Different current densities (0.1, 0.3, 0.5, 0.8, 1.0, 2.0, 3.0 mA cm^{-2}) were applied to the coin cell and the cell voltages were recorded.

3. Results and discussions

3.1 Preparation of chitosan hydrogel membranes (CS-HGMs)

Figure 1A illustrates the chitosan hydrogel membranes fabrication process. The reaction occurring between chitosan and acetic acid in aqueous solution as it dissolves is also depicted. The main functional group present in each monomer unit of chitosan is the amine group ($–NH_2$), and the remaining structural moiety is represented by R which is comprised of a six-membered ring structure, containing an ether group and a primary alcohol group attached to its backbone. [33] This reaction in acid results in the protonation of the $–NH_2$ group of chitosan to form $–NH_3^+$ which can then be converted back to $–NH_2$ by air drying when the organic acid is removed by evaporation. [32] The modifications using SiO_2, SnO_2, and ZnO can change the hardness of chitosan-based hydrogel membranes with increasing hardness as follows: CS-HGM < SiO_2-CS-HGM < SnO_2-CS-HGM < ZnO-CS-HGM. After equilibrating in a 2 M aqueous NaOH

solution, the swelling of dry HGMs occurs. The topographies of 10%-SiO_2-CS, 10%-SnO_2-CS, and 10%-ZnO-CS HGMs before and after equilibrating in alkaline solution are respectively shown in **Figure 1B**.

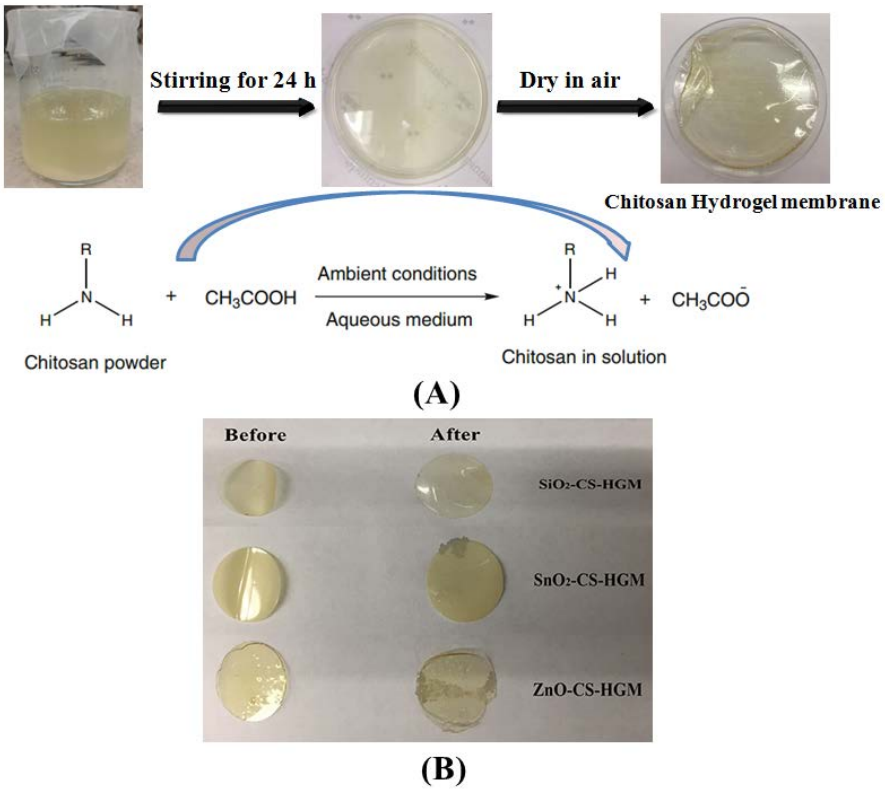

Figure 1. (A) Schematic of CS-HGM preparation; (B) SiO_2, SnO_2, and ZnO-CS-HGM before and after equilibrating in 2 M aqueous NaOH solution.

3.2 Ionic conductivity studies

The ac impedance spectra for the CS-HGMs are shown in **Figure 2**. The impedance spectra have two typical well-defined regions. The arcs in the high frequency range correspond to the ionic conduction process in the CS-HGMs. The lines parallel to the imaginary axis in the low frequency range are ascribed to the effect of the mixed electrode and electrolyte interface. The room temperature ionic

conductivity values of CS-HGMs are calculated based on their wet thicknesses and resistances, which are presented in **Table 1**. It can be concluded that 10%-SiO_2-CS-HGM has the highest ionic conductivity among all the prepared HGMs.

The high ionic conductivity of CS-HGMs in alkaline medium may be attributed to a higher water uptake capacity of chitosan. [33] Greater water uptake ability of CS-HGM leads to greater uptake ability of KOH electrolytes, and ultimately contributes to a higher ionic conductivity due to the greater number and mobility of ions in the polymer complexes. [39] In addition, OH^- ions from the KOH solution are capable of forming hydrogen bonds with water in the CS hydrogel matrix and can be transported through the matrix by a Grotthus type mechanism. [40] The polar functional groups of CS, such as –OH, $–NH_2$, and C–O–C groups also form hydrogen bonds with water, and can therefore trap water molecules in its polymer matrix. [41] Interestingly, the ionic conductivities of CS-HGMs containing metal oxides are higher than those of pure CS HGMs, suggesting that the modifications of SiO_2, SnO_2, and ZnO fillers can improve the ionic conductivity due to the incidental formations of SiO_3^{2-}, SnO_3^{2-}, and $Zn(OH)_4^{2-}$ ions, which may also act as corrosion inhibitors for Al anode. The low conductivity of 15%-SiO_2-CS-HGM may be attributed to the increased amount of SiO_2 reacting with KOH (Equation 2-2), which decreases the proportion of effective OH^- charge carriers. The SEM image in **Figure 3** shows the existence of particles in 10%-SiO_2-CS-HGM. Elemental mapping confirms that the homogeneous distributed particles are SiO_2.

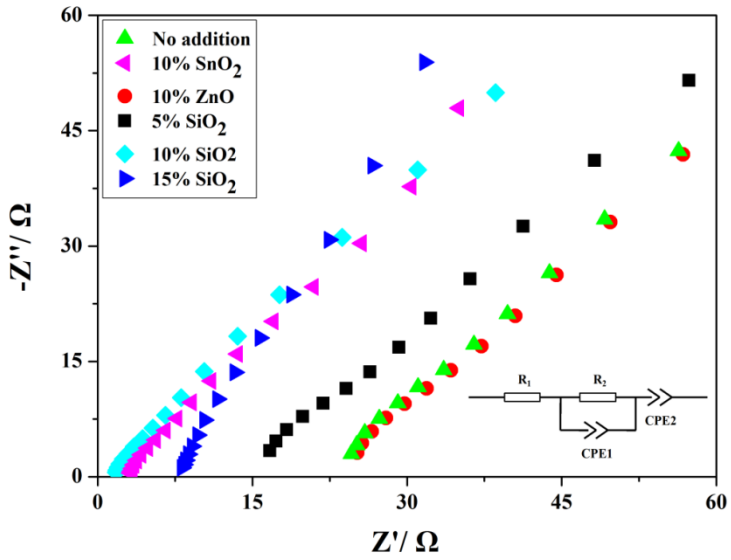

Figure 2. Nyquist plots of chitosan-based hydrogel membranes (CS-HGMs). The quivalent-circuit model is shown in the insert.

Table 1. Resistances, wet thicknesses, and room temperature ionic conductivities of CS-HGMs.

	Pristine	+10% SnO_2	+10% ZnO	+ 5% SiO_2	+10% SiO_2	+15% SiO_2
R (Ω)	17.46	11.80	10.34	30.57	68.66	67.89
Thickness (cm)	0.15	0.22	0.29	0.15	0.16	0.17
Ionic conductivity (S cm^{-1})	2.32×10^{-5}	2.05×10^{-4}	4.65×10^{-5}	5.14×10^{-5}	1.52×10^{-4}	9.00×10^{-5}

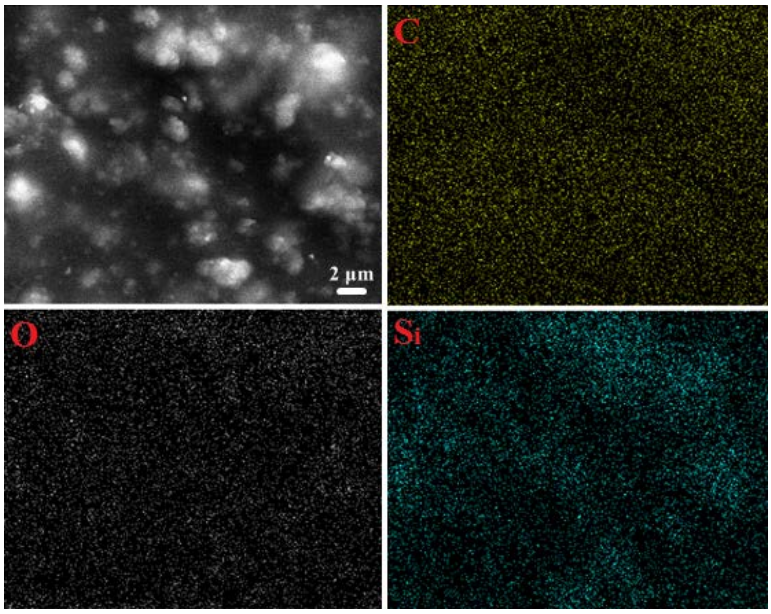

Figure 3. The SEM image and elemental mapping images of C, O and Si in the 10%-SiO_2-CS-HGM.

3.3 Electrochemical performance of Al-air coin cell using CS-HGMs as separators

The Al-air coin cell is fabricated with the chitosan-based membrane and glass fiber sandwiched between the Mn_3O_4/C cathode and Al alloy anode, as shown schematically in **Figure S1**. The electrochemical catalytic activity of the Mn_3O_4/C air electrode was evaluated. The LSV curves in O_2-saturated 0.1 M KOH electrolyte at various rotation rates (400, 625, 900, 1225, and 1600 rpm) with a scan rate of 5 mV s^{-1} (**Fig. S2a**) and the corresponding Koutecky-Levich (K-L) plots at different potentials (**Figure S2b)** were obtained to understand the ORR performance of the Mn_3O_4/C catalyst. The *n* of the Mn_3O_4/C catalyst is calculated to be about 3.18, suggesting good electrocatalytic activity for ORR.

Figure 4 shows the discharge behaviors of the coin cells using CS, 5%-, 10%-,

15%-SiO_2-CS, 10%-SnO_2-CS, and 10%-ZnO-CS HGMs as separators at a constant current density of 1.0 mA cm^{-2} under ambient conditions. The coin cell assembled with 10%-SiO_2-CS-HGM exhibits an open circuit voltage of 1.43 V, which is higher than that of other membranes, which can be consistent with the ionic conductivity characterization results on the CS-HGMs. Moreover, it is obvious that the discharge duration and flat plateau of the coin cell assembled with 10%-SiO_2-CS-HGM perform better than those of the cells assembled with other CS-HGMs. The discharge time of the coin cell with 10%-SiO_2-CS-HGMs is up to 8000s, which is longer than that of the coin cells with other membranes, indicating the 10%-SiO_2-CS-HGMs can improve the stability of the coin cell. The summary of discharge performance of Al-air cells using different CS-HGMs were tabulated in **Table 2**. The discharge performance of the coin cells assembled with CS-HGMs increases as follows: 10%-ZnO-CS-HGMs < CS-HGMs < 5%-SiO_2-CS-HGMs < 10%-SnO_2-CS-HGMs < 15%-SiO_2-CS-HGMs < 10%-SiO_2-CS-HGMs. These results indicate that the presence of SiO_2 and SnO_2 in chitosan membranes can enhance the discharge performance of the coin cells by contributing to the formation of SiO_3^{2-} and SnO_3^{2-} which act as corrosion inhibitors in the Al-air system in alkaline condition. [7, 42-44] The corrosion inhibitors can effectively inhibit the corrosion and hydrogen evolution process of Al anode. The discharge duration is determined by the utilization of Al anode. The formative corrosion inhibitors can mitigate the corrosion of Al, raise the overpotential of hygrogen evolution, and extend the lifetime of coin cells. The better discharge performance of the coin cell with 10%-SiO_2-CS-HGM may be attributed to its higher corrosion

inhibition and ionic conductivity compared to other CS-HGMs. However, the formation of $Zn(OH)_4^{2-}$ plays a negative effect on the performance of Al-air coin cell, which may be contributed to the inferior corrosion inhibition of $Zn(OH)_4^{2-}$ and its high consumption of electrolyte.

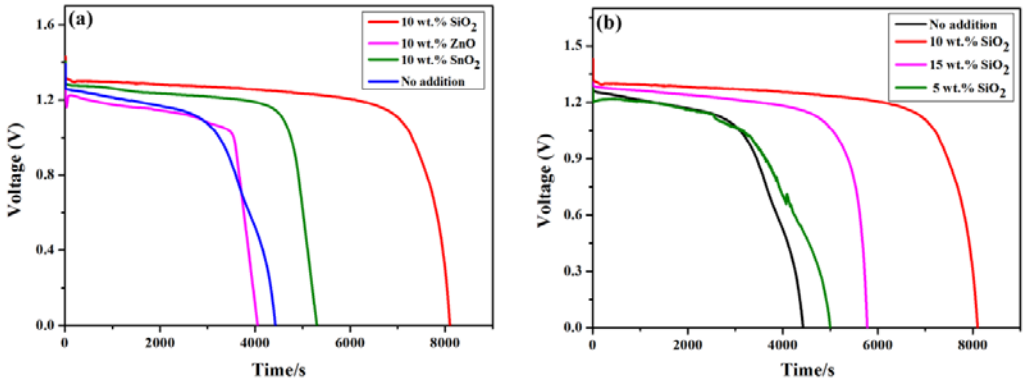

Figure 4. Discharge performance of the Al–air coin cells with (a) different CS-HGMs, (b) SiO_2-CS-HGMs with different mass ratios of SiO_2 and chitosan.

Table 2. The summary of discharge performance of the coin cells assembled with CS-HGMs at a current density of 1.0 mA cm^{-2} under ambient conditions.

Sample	Open circuit voltage (V)	Flat plateau (V)	Discharge time (s)
CS-HGM	1.34	1.20	4055
5% SiO_2-CS-HGM	1.39	1.20	4997
10% SiO_2-CS-HGM	1.43	1.30	8102
15% SiO_2-CS-HGM	1.39	1.28	5778
10% SnO_2-CS-HGM	1.40	1.28	5301
10% ZnO-CS-HGM	1.38	1.18	4425

Figure S3 presents the morphology change of the Mn_3O_4/C catalyst before and

after the discharge test. It is obvious that the Mn_3O_4/C catalyst has almost no visible change after discharge compared to its initial state, indicating good stability of the Mn_3O_4/C catalyst during electrochemical cycling. This also suggests that there is a possibility that it can be reused in a new Al-air cell, which will be demonstrated in the last section of this study. In order to further study the corrosion inhibition of the chitosan-based membranes, we observed the surface morphologies of Al alloy anodes in the coin cells assembled with different membranes after a 90 min discharge at a constant current density of 1.0 mA cm^{-2}, as shown in **Figure 5**. The surface topography of the pristine Al alloy is presented in **Figure S4**. At equilibrium conditions, the oxidation product of Al in strong alkaline solution is soluble $Al(OH)_3$. Dissolved $Al(OH)_4^-$ ions near the electrode precipitate on the aluminum surface and transform into a $Al(OH)_3$ layer or defective Al_2O_3. [45] The surface morphology of the Al alloy in the cell with CS-HGMs after discharge exhibits more intense corrosion and the passivation layer is thicker (**Figure 5a**). The surface of the Al alloy in the cell with SiO_2-CS-HGMs is smoother and shallow pits were observed in **Figure 5b**, which should be due to the increase in the rate of dissolution of $Al(OH)_3$ layer. The corrosion degree of the Al alloys in the cells with CS-HGMs increases as follows: SiO_2-CS-HGM < SnO_2-CS-HGM < ZnO-CS-HGM, suggesting SiO_2-CS-HGM is the most effective at inhibiting the corrosion (electrochemical consumption) of the Al alloy, i.e. a better utilization of Al anode.

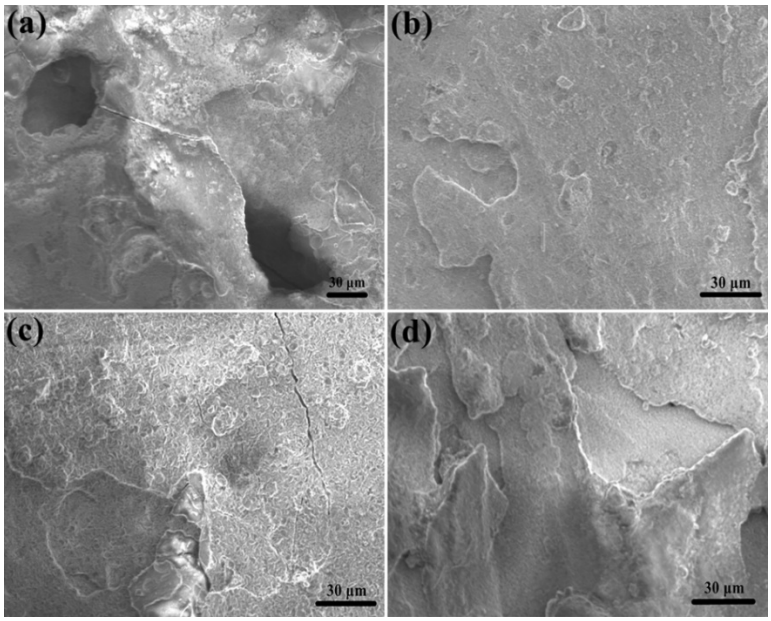

Figure 5. SEM images of the Al alloy anodes in the cells assembled with CS-HGMs: (a) CS-HGM, (b) SiO_2-CS-HGM, (c) SnO_2-CS-HGM, and (d) ZnO-CS-HGM after discharge tests.

Figure 6a,b presents typical galvanostatic discharge profiles at different current densities for the coin cells with 10%-SiO_2-CS-HGMs as separators and pure Al foil anodes (99.9999%, ~ 0.025 mm thick, 1 cm × 1cm). The duration of the discharge process decreases approximately linearly with increasing current density, suggesting the similar utilization degree of Al. The fluctuation of the voltage curve was due to the gradual corrosion and degradation of the Al anode. Generally, the voltage plateau dropped correspondingly as the current density increased from 0.1 to 1.0 mA cm^{-2} due to the increased cell polarization. The specific capacity normalized to the mass of consumed Al is 36.5, 165.5, and 288.5 mAh g^{-1} at current densities of 0.1, 0.5, and 1.0 mA cm^{-2}, respectively. In fact, the Al-air coin cell with 10% SiO_2-CS-HGM had a capacity of 1.15 mAh cm^{-2} at the areal current density of 1.0 mA cm^{-2}.

In order to evaluate the practical performance of the coin cells, the cell polarization and power density curves of coin cells with SiO_2-CS, SnO_2-CS, and ZnO-CS HGMs were recorded, as shown in **Figure 7**. The plateau voltages ranged between 1.48 and 1.17 V with an applied discharge current density in the range of 0.1 to 3.0 mA cm^{-2}. With the increase of current density, the discharge plateau voltage decreases accordingly. The Al-air coin cells with 10%-SiO_2-CS, 10%-SnO_2-CS, and 10%-ZnO-CS HGMs as separators have the peak power densities (P_{max}) of 3.8, 2.8, and 2.5 mW cm^{-2}, respectively. The coin cell with SiO_2-CS-HGM exhibits the highest power density, suggesting that SiO_2-CS-HGM can be used as a promising separator in Al-air coin cells.

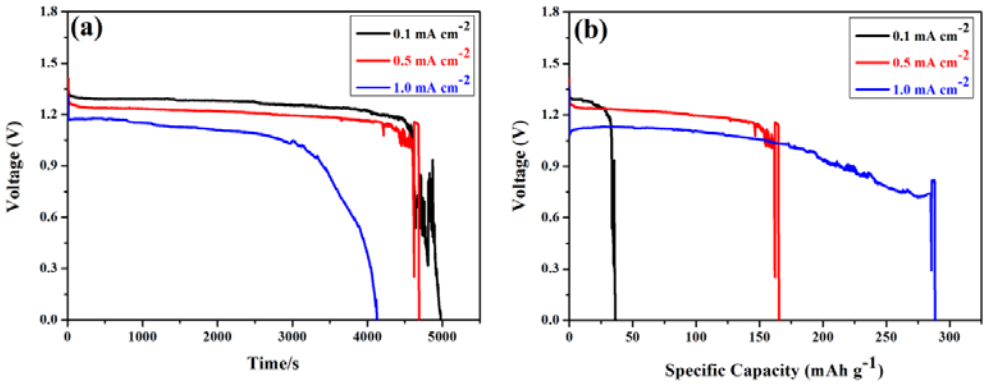

Figure 6. (a, b) Discharge curves for the Al–air coin cell with 10%-SiO_2-HGM at current densities of 0.1, 0.5, and 1.0 mA cm^{-2}.

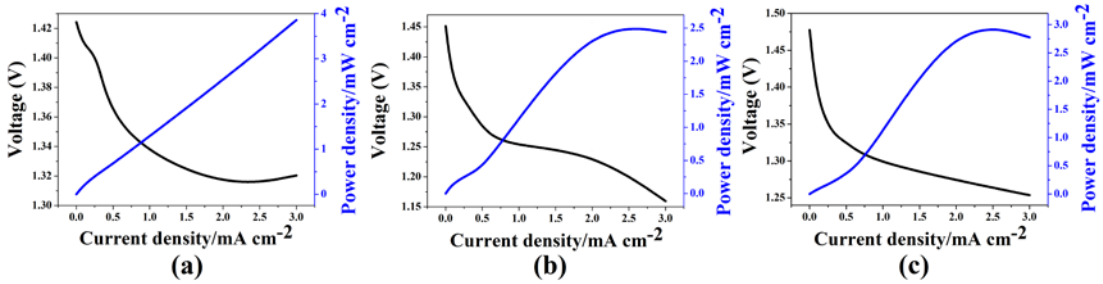

Figure 7. Cell polarization and power density plots for the Al-air coin cells with (a) 10%-SiO_2-CS, (b) 10%-SnO_2-CS, and (c) 10%-ZnO-CS HGMs.

3.4 Comparison of chitosan hydrogel membrane with other hydrogel membranes

To demonstrate the superiority of CS-HGMs, other hydrogel membranes were also prepared. The two reported polysaccharides of xanthan and gelatin as starting solid matrices in KOH solutions were synthsized for comparison. Xanthan gum is a bacterial polysaccharide commercially produced by secretion from the bacterium *Xanthomonas campestris* in aerobic fermentation conditions. [46] Gelatin is a water-soluble denatured protein obtained either by partial acid or alkaline hydrolysis of animal collagen. [47] They have been extensively used as starting solid matrices to prepare hydrogels as solid state electrolytes for electrochemical devices, such as batteries and fuel cells. [48-49] However, to the best of our knowledge, xanthan has been just reported as solid electrolytes in Al-air primary batteries, [46] no data are available in literature for Al-air coin cell. Xanthan in this reference has been prepared as a paste-like gel and directly used as solid electrolyte. The Al-air primary battery is an all-solid-state battery with a capacity of 0.76 mAh cm^{-2} at the current density of 1.0 mA cm^{-2}. In this study, xanthan and gelatin membranes (**Figure S5**) were used as separators in Al-air coin cell, with the preparation method and product characteristics listed in **Table S1**. The discharge curves of coin cells with chitosan, xanthan and

gelatin membranes at 1.0 mA cm^{-2} are shown in **Figure S6**. The best performance was obtained with the hydrogel membrane prepared using chitosan, in terms of higher voltage plateau, longer discharge duration and higher energy density, which is attributed to the partially dissolution of xanthan and gelatin membranes and the stability of chitosan membranes in alkaline condition of Al-air coin cells. The results suggest that chitosan membranes are more valuable for use in Al-air coin cells.

3.5 Eco-friendly recycling procedure of Al-air coin cells

Recycling and chemical waste disposal are common challenges for state-of-the-art coin cell systems. In this work, we made use of a series of eco-friendly procedures to recycle the components of Al-air coin cells after discharge. The Al-air coin cell was fabricated as described in section 2.3, except a 1 cm × 1 cm battery-grade pure aluminum foil (99.9999%, ~ 0.025 mm in thick) was used as the anode instead. The coin cell is primarily composed of five components: (1) a Mn_3O_4/C based freestanding cathode; (2) a chitosan membrane; (3) a pure Al foil anode; (4) a 12 mm diameter sheet of hydrophobic carbon paper as a waterproof cover; and (5) a commercial stainless steel coin cell shell and gasket. After discharge, $Al(OH)_3$ exists as the discharge product in the cell.

Figure 8A, B is a flow diagram and schematic image describing the recycling process of an Al-air coin cell, involving only food-grade ingredients, which can be perform using household items such as paper cups, funnels, and coffee filters (**Figure S7**). The first step is to treat the discharged Al-air cell with 10% (v/v) acetic acid solution, or white vinegar. The chitosan membrane can be completely dissolved in this

acid solution within 1 h. The acetic acid solution was then filtered using filter paper and a funnel. The Mn_3O_4/C cathode and carbon paper can be easily collected and recycled to be used in a new Al-air coin cell after drying. The discharge performance of the coin cells with a new recycled cathode was compared in **Figure S8**. The relatively stable voltage plateau, discharge duration, and specific capacity in the coin cells indicate excellent stability and recyclability of the cathode. Meanwhile, the $Al(OH)_3$ on the surface of unexhausted Al foil can be completely dissolved in 10% acetic acid solution within 12 h. The polished Al foil can then be recycled as well. In order to avoid contaminating the water system with Al^{3+} ions, an equivalent amount of sodium bicarbonate ($NaHCO_3$), or baking soda, was added into the filtrate to neutralize the acetic acid and precipitate the Al^{3+} ions. Once, the secondary filtrate is neutralized, it is environmentally safe and can be arbitrarily disposed.

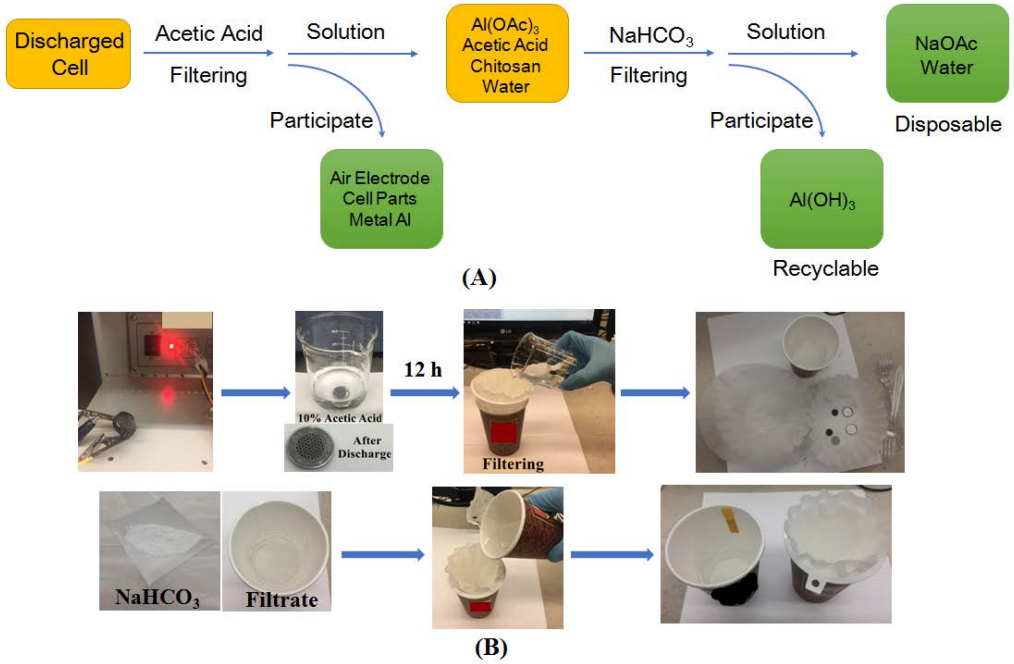

Figure 8. (A) The flow diagram and (B) schematic image of the recycling procedure of a discharged Al-air coin cell and acidic filtrate.

4. Conclusions

To summarize, we have demonstrated the fabrication and characterization of Al-air coin cells using eco-friendly chitosan hydrogel membranes, which shows superior electrochemical performance and can be easily recycled. The influences of metal oxides fillers (SiO_2, SnO_2, and ZnO) and the content of SiO_2 on the cell performance were then investigated and optimized. The discharge tests showed that the electrochemical consumption of Al alloy anode is more uniform when using 10%-SiO_2-CS-HGM as a separator, and the specific capacity of the cell with 10%-SiO_2-CS-HGM can reach up to 288.5 mAh g^{-1} at a current density of 1.0 mA cm^{-2}. The improved performance of Al-air cells using SiO_2-CS-HGM can be also attributed to the generation of SiO_3^{2-} which acts as a corrosion inhibitor via the reaction between SiO_2 and KOH. Additionally, the components of the Al-air coin cell after discharge can be completely recycled using environmentally safe procedures with only household items. We believe this new design for potable and recyclable coin-type Al–air batteries may open up new applications in small-size electronics.

The Supporting Information is available:

The configuration of an Al-air coin cell; K-L equation to calculate the electron transfer number (*n*), LSV curves and K-L plots; SEM images of Mn_3O_4/C catalyst; SEM images of the surface topography of Al alloy anode; One image of xanthan and gelatin powers and membranes; One table listing the preparation method and characteristics of hydrogels prepared from xanthan and gelatin polysaccharides;

Discharge curves of Al-air coin cells using the three hydrogels; One image of recycling tools; Discharge performance of Al–air coin cells with a new cathode and a recycled cathode.

Acknowledgements

This research was supported by the Natural Sciences and Engineering Research Council of Canada, Canada Research Chair Program, National Nature Science Foundation of China (No.51474255), and Open-End Fund for the Graduate Student Research Innovation Project of Hunan Province (No. 150140008).

References

1. Girishkumar G.; McCloskey B.; Luntz A. C.; Swanson S.; Wilcke W., Lithium−Air Battery: Promise and Challenges. *J. Phys. Chem. Lett.*, 2010, **1**, 2193-2203.
2. Li, C.-S.; Sun, Y.; Gebert, F.; Chou, S.-L., Current Progress on Rechargeable Magnesium-Air Battery. *Adv. Energy Mater.* **2017**, 7, 1700869-1700880.
3. Tan, P.; Chen, B.; Xu, H.; Zhang, H.; Cai, W.; Ni, M.; Liu, M.; Shao, Z., Flexible Zn– and Li–Air Batteries: Recent Advances, Challenges, and Future Perspectives. *Energy Environ. Sci.* **2017**, 10, 2056-2080.
4. Liu, Y.; Sun, Q.; Li, W.; Adair, K. R.; Li, J.; Sun, X., A Comprehensive Review on Recent Progress in Aluminum–Air Batteries. *Green Energy & Environ.* **2017,** 2, 246-277.
5. Kapali, V.; Lyer, S. V.; Balaramachandran, V.; Sarangapani, K. B.; Ganesan, M.; Kulandainathan, M. A.; Mideen, A. S., Studies on the Best Alkaline Electrolyte for Aluminium/Air Batteries. *J. Power Sources* **1992**, 39, 263-269.
6. Mori, R., Electrochemical Properties of A Rechargeable Aluminum–Air Battery with a Metal–Organic framework as air cathode material. *RSC Adv.* **2017,** 7, 6389-6395.
7. Mokhtar, M.; Talib, M. Z. M.; Majlan, E. H.; Tasirin, S. M.; Ramli, W. M. F. W.; Daud, W. R. W.; Sahari, J., Recent Developments in Materials for Aluminum–Air Batteries: A Review. *J. Ind. Eng. Chem.* **2015,** 32, 1-20.
8. Wang, Y.-J.; Qiao, J.; Baker, R.; Zhang, J., Alkaline Polymer Electrolyte Membranes for Fuel Cell Applications. *Chem. Soc. rev.* **2013,** 42, 5768-5787.

9. Kim, D. J.; Jo, M. J.; Nam, S. Y., A Review of Polymer–Nanocomposite Electrolyte Membranes for Fuel Cell Application. *J. Ind. Eng. Chem.* **2015,** 21, 36-52.
10. Ketpang, K.; Lee, K.; Shanmugam, S., Facile Synthesis of Porous Metal Oxide Nanotubes and Modified Nafion Composite Membranes for Polymer Electrolyte Fuel Cells Operated Under Low Relative Humidity. *ACS Appl. Mater. Interfaces* **2014,** 6, 16734-44.
11. Ketpang, K.; Oh, K.; Lim, S.-C.; Shanmugam, S., Nafion-Porous Cerium Oxide Nanotubes Composite Membrane for Polymer Electrolyte Fuel Cells Operated Under Dry Conditions. *J. Power Sources* **2016,** 329, 441-449.
12. Milikić, J.; Ćirić-Marjanović, G.; Mentus, S.; Santos, D. M. F.; Sequeira, C. A. C.; Šljukić, B., Pd/c-PANI Electrocatalysts for Direct Borohydride Fuel Cells. *Electrochim. Acta* **2016,** 213, 298-305.
13. Guo, S.; Sun, J.; Zhang, Z.; Sheng, A.; Gao, M.; Wang, Z.; Zhao, B.; Ding, W., Study of the Electrooxidation of Borohydride on a Directly Formed CoB/Ni-Foam Electrode and Its Application in Membraneless Direct Borohydride Fuel Cells. *J. Mater. Chem. A* **2017,** 5, 15879-15890.
14. Dutta, K.; Das, S.; Kundu, P. P., Partially Sulfonated Polyaniline Induced High Ion-Exchange Capacity and Selectivity of Nafion Membrane for Application in Direct Methanol Fuel Cells. *J. Membrane Sci.* **2015,** 473, 94-101.
15. Sha Wang, L.; Nan Lai, A.; Xiao Lin, C.; Gen Zhang, Q.; Mei Zhu, A.; Lin Liu, Q., Orderly Sandwich-Shaped Graphene Oxide/Nafion Composite Membranes for Direct Methanol Fuel Cells. *J. Membrane Sci.* **2015,** 492, 58-66.
16. Wu, W.; Li, Y.; Liu, J.; Wang, J.; He, Y.; Davey, K.; Qiao, S. Z., Molecular-Level Hybridization of Nafion with Quantum Dots for Highly Enhanced Proton Conduction. *Adv. Mater.s* **2018,** 30, 1707516-1707522.
17. Cheng, H.; Scott, K.; Lovell, K. V.; Horsfall, J. A.; Waring, S. C., Evaluation of New Ion Exchange Membranes for Direct Borohydride Fuel Cells. *J. Membrane Sci.* **2007,** 288, 168-174.
18. Ma, J.; Choudhury, N. A.; Sahai, Y.; Buchheit, R. G., Performance Study of Direct Borohydride Fuel Cells Employing Polyvinyl Alcohol Hydrogel Membrane and Nickel-Based Anode. *Fuel Cells* **2011,** 11, 603-610.
19. An, L.; Zhao, T. S.; Zeng, L., Agar Chemical Hydrogel Electrode Binder for Fuel-Electrolyte-Fed Fuel Cells. *Appl. Energy* **2013,** 109, 67-71.
20. Kamath, K. R.; Park, K., Biodegradable Hydrogels in Drug Delivery. *Adv. Drug Delivery Rev.* **1993,** 11, 59-84.
21. Panero, S.; Fiorenza, P.; Navarra, M. A.; Romanowska, J.; Scrosati, B., Silica-Added, Composite Poly(vinyl alcohol) Membranes for Fuel Cell Application. *J. Electrochem. Soc.* **2005,** 152, A2400-A2405.
22. Choudhury, N. A.; Shukla, A. K.; Sampath, S.; Pitchumani, S., Cross-Linked Polymer Hydrogel Electrolytes for Electrochemical Capacitors. *J. Electrochem. Soc.* **2006,** 153, A614-A620.
23. Sahu, A. K.; Selvarani, G.; Pitchumani, S.; Sridhar, P.; Shukla, A. K.; Narayanan, N.; Banerjee, A.; Chandrakumar, N., PVA-PSSA Membrane with Interpenetrating Networks and its Methanol Crossover Mitigating Effect in DMFCs. *J. Electrochem.*

Soc. **2008,** 155, B686-B695.
24. Wilson, M. S., U.S. Patent 5,234,777[P]. 1993-8-10.
25. Xu, Y.; Zhang, Y.; Guo, Z.; Ren, J.; Wang, Y.; Peng, H., Flexible, Stretchable, and Rechargeable Fiber-Shaped Zinc-Air Battery Based on Cross-Stacked Carbon Nanotube Sheets. *Angew. Chem. Int. Ed. Engl.* **2015,** 54, 15390-15394.
26. Xu, Y.; Zhao, Y.; Ren, J.; Zhang, Y.; Peng, H., An All-Solid-State Fiber-Shaped Aluminum-Air Battery with Flexibility, Stretchability, and High Electrochemical Performance. *Angew. Chem. Int. Ed. Engl.* **2016,** 55, 7979-7982.
27. Zeng, Y.; Zhang, X.; Meng, Y.; Yu, M.; Yi, J.; Wu, Y.; Lu, X.; Tong, Y., Achieving Ultrahigh Energy Density and Long Durability in a Flexible Rechargeable Quasi-Solid-State Zn-MnO_2 Battery. *Adv. Mater.* **2017,** 29, 1700274-1700210.
28. Finkenstadt, V. L., Natural polysaccharides as electroactive polymers. *Appl.Microbiolo. Biot.* **2005,** 67, 735-45.
29. Kadokawa, J.-i.; Murakami, M.-a.; Takegawa, A.; Kaneko, Y., Preparation of Cellulose–Starch Composite Gel and Fibrous Material From a Mixture of the Polysaccharides in Ionic Liquid. *Carbohyd. Polym.* **2009,** 75, 180-183.
30. YOSHIDA, H.; TAKEI F.; SAWATARI, N., High Ionic Conducting Polymer with Polysaccharide and Its Applications. Fujitsu: Kawasaki, JAPON, **2002**; Vol. 38, p 7.
31. Wan, Y.; Creber, K. A. M.; Peppley, B.; Bui, V. T., Ionic Conductivity of Chitosan Membranes, *Polymer* **2003**, 44, 1057-1065.
32. Choudhury, N. A.; Sahai, Y.; Buchheit, R. G., Chitosan Chemical Hydrogel Electrode Binder for Direct Borohydride Fuel Cells. *Electrochem. Commun.* **2011,** 13, 1-4.
33. Ma, J.; Sahai, Y.; Buchheit, R. G., Evaluation of Multivalent Phosphate Cross-Linked Chitosan Biopolymer Membrane for Direct Borohydride Fuel Cells. *J. Power Sources* **2012,** 202, 18-27.
34. Wang, D.; Tang, X.; Qiu, Y.; Gan, F.; Zheng Chen, G., A Study of the Film Formation Kinetics on Zinc in Different Acidic Corrosion Inhibitor Solutions by Quartz Crystal Microbalance. *Corros. Sci.* **2005,** 47, 2157-2172.
35. Macdonald, D. D.; English, C., Development of Anodes for Aluminium/Air Batteries—Solution Phase Inhibition of Corrosion. *J. Appl. Electrochem.* **1990**, 20, 405-417.
36. Lopez-Garrity, O.; Frankel, G. S., Corrosion Inhibition of AA2024-T3 By Sodium Silicate. *Electrochim. Acta* **2014,** 130, 9-21.
37. Wang, J.; Chen, P.; Shi, B.; Guo, W.; Jaroniec, M.; Qiao, S. Z., A Regularly Channeled Lamellar Membrane for Unparalleled Water and Organics Permeation. *Angew. Chem. Int. Ed. Engl.* **2018,** 57, 1-6.
38. Guan, J.; Zhang, Z.; Ji, J.; Dou, M.; Wang, F., Hydrothermal Synthesis of Highly Dispersed Co_3O_4 Nanoparticles on Biomass-Derived Nitrogen-Doped Hierarchically Porous Carbon Networks as an Efficient Bifunctional Electrocatalyst for Oxygen Reduction and Evolution Reactions. *ACS Appl. Mater. Interfaces* **2017**, 9, 30662-30669.
39. Du, J. F.; Bai, Y.; Chu, W. Y.; Qiao, L. J., The Structure and Electric Characters of Proton-Conducting Chitosan Membranes with Various Ammonium Salts as

Complexant. *J. Polym. Sci. Pol. Phys.* **2010,** 48, 880-885.
40. Singh, A.; Narvi, S. S.; Dutta, P. K.; Pandey, N. D., External Stimuli Response on a Novel Chitosan Hydrogel Crosslinked with Formaldehyde. *B. Mater. Sci*. **2006**, 29, 233-238.
41. Choudhury, N. A.; Ma, J.; Sahai, Y.; Buchheit, R. G., High Performance Polymer Chemical Hydrogel-Based Electrode Binder Materials for Direct Borohydride Fuel Cells. *J. Power Sources* **2011,** 196, 5817-5822.
42. Liu, J.; Wang, D.; Zhang, D.; Gao, L.; Lin, T., Synergistic Effects of Carboxymethyl Cellulose and ZnO as Alkaline Electrolyte Additives for Aluminium Anodes with a View towards Al-Air Batteries. *J. Power Sources* **2016,** 335, 1-11.
43. Rashvand avei, M.; Jafarian, M.; Moghanni Bavil Olyaei, H.; Gobal, F.; Hosseini, S. M.; Mahjani, M. G., Study of the Alloying Additives and Alkaline Zincate Solution Effects on the Commercial Aluminum as Galvanic Anode for Use in Alkaline Batteries. *Mater. Chem. Phys.* **2013,** 143, 133-142.
44. Egan, D. R.; Ponce de León, C.; Wood, R. J. K.; Jones, R. L.; Stokes, K. R.; Walsh, F. C., Developments in Electrode Materials and Electrolytes for Aluminium–Air batteries. *J. Power Sources* **2013,** 236, 293-310.
45. Chen, B.; Leung, D. Y. C.; Xuan, J.; Wang, H., A High Specific Capacity Membraneless Aluminum-Air Cell Operated with an Inorganic/Organic Hybrid Electrolyte. *J. Power Sources* **2016,** 336, 19-26.
46. Di Palma, T. M.; Migliardini, F.; Caputo, D.; Corbo, P., Xanthan and κ-carrageenan Based Alkaline Hydrogels as Electrolytes for Al/Air Batteries. *Carbohyd. Polym.* **2017,** 157, 122-127.
47. Aviv-Gavriel, M.; Garti, N.; Furedi-Milhofer, H., Preparation of a Partially Calcified Gelatin Membrane as a Model for a Soft-to-Hard Tissue Interface. *Langmuir : ACS J. surfaces and colloids* **2013,** 29, 683-9.
48. Wong, C. Y.; Wong, W. Y.; Loh, K. S.; Mohamad, A. B., Study of the Plasticising Effect on Polymer and Its Development in Fuel Cell Application. *Renew. Sustain. Energy Rev.* **2017,** 79, 794-805.
49. Park, J.; Park, M.; Nam, G.; Lee, J. S.; Cho, J., All-Solid-State Cable-Type Flexible Zinc-Air Battery. *Adv. Mater.* **2015,** 27, 1396-401.

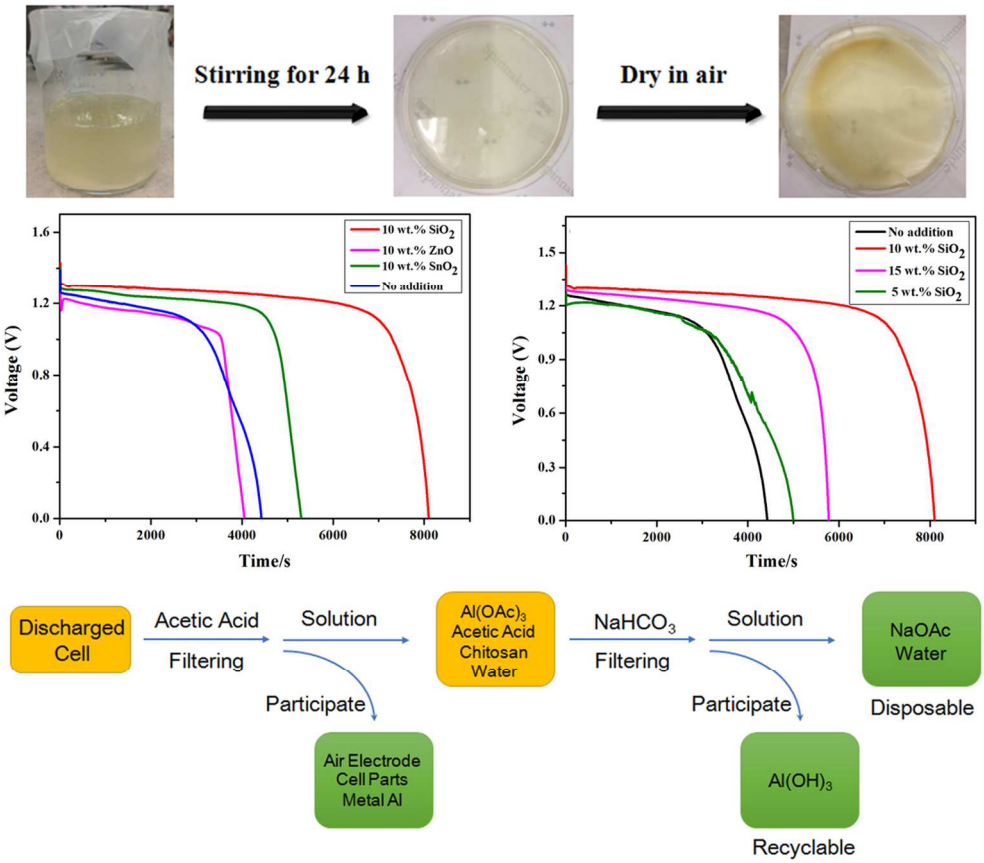

110x95mm (300 x 300 DPI)